

# Carbon–Carbon Bond-Forming Reductive Elimination from Isolated Nickel(III) Complexes

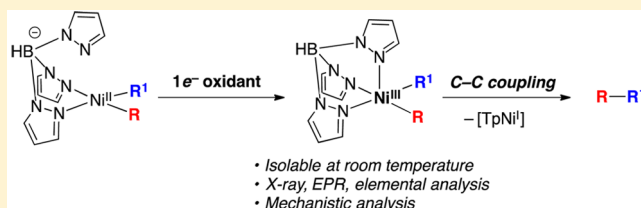
James R. Bour,<sup>†</sup> Nicole M. Camasso,<sup>†</sup> Elizabeth A. Meucci,<sup>†</sup> Jeff W. Kampf,<sup>†</sup> Allan J. Canty,<sup>‡</sup> and Melanie S. Sanford<sup>\*,†,§</sup>

<sup>†</sup>Department of Chemistry, University of Michigan, 930 N. University Avenue, Ann Arbor, Michigan 48109, United States

<sup>‡</sup>School of Physical Sciences, University of Tasmania, Hobart, Tasmania 7001, Australia

## Supporting Information

**ABSTRACT:** This manuscript describes the design, synthesis, characterization, and reactivity studies of organometallic Ni<sup>III</sup> complexes of general structure TpNi<sup>III</sup>(R)(R') (Tp = tris(pyrazolyl)borate). With appropriate selection of the R and R' ligands, the complexes are stable at room temperature and can be characterized by cyclic voltammetry, EPR spectroscopy, and X-ray crystallography. Upon heating, many of these Ni<sup>III</sup> compounds undergo C(sp<sup>2</sup>)–C(sp<sup>2</sup>) or C(sp<sup>3</sup>)–C(sp<sup>2</sup>) bond-forming reactions that are challenging at lower oxidation states of nickel.



## INTRODUCTION

Nickel-catalyzed cross coupling has emerged as an economical and often complementary alternative to more conventional palladium-catalyzed methods.<sup>1</sup> The propensity of nickel to undergo single electron redox events enables catalytic manifolds that are mechanistically distinct from those at palladium.<sup>2</sup> In many Ni-catalyzed reactions, the product-forming step is believed to involve C–C bond-forming reductive elimination from a transient Ni<sup>III</sup> intermediate bearing two carbon donor ligands.<sup>3</sup> Despite the ubiquity of this proposed mechanism, examples of isolated diorganonickel(III) complexes remain extremely rare.<sup>4–6</sup> As such, this key step of the catalytic cycle has largely eluded direct interrogation.

The vast majority of work on the organometallic chemistry of Ni<sup>III</sup> has focused on complexes bearing a single aryl or alkyl donor ligand.<sup>7</sup> A variety of such complexes have been characterized in situ and/or isolated,<sup>2c,8–10</sup> and their reactivity with various heteroatom and carbon nucleophiles has been studied. In marked contrast, examples of more catalytically relevant diorganonickel(III) complexes have remained elusive until very recently. Early work by Kochi implicated transient [Ni<sup>III</sup>(R)(R')] intermediates in Ni-mediated C(sp<sup>2</sup>)–C(sp<sup>2</sup>) coupling reactions.<sup>2a</sup> However, these intermediates were only inferred from reactivity studies and low temperature cyclic voltammetry<sup>10</sup> and were not directly observed or structurally characterized. More than three decades later, Mirica demonstrated that a tetradentate nitrogen donor ligand can be used to support a detectable Ni<sup>III</sup>(CH<sub>3</sub>) (aryl) intermediate.<sup>5</sup> However, this complex was only characterized in situ using EPR and mass spectrometry. Upon warming from –50 °C to room temperature, it underwent C(sp<sup>2</sup>)–C(sp<sup>3</sup>) bond-forming reductive elimination. Finally, very recently, Mirica has used a closely related tetradentate ligand scaffold to generate an isolable Ni<sup>III</sup>

dimethyl complex that undergoes ethane reductive elimination over 12 h in MeCN at room temperature.<sup>4</sup>

We aimed to develop a strategy for the synthesis of isolable Ni<sup>III</sup> complexes of general structure L<sub>n</sub>Ni<sup>III</sup>(R)(R'), such that we could conduct detailed studies of their reactivity. We report herein that the facial tridentate tris(pyrazolyl)borate ligand supports a variety of isolable Ni<sup>III</sup> complexes (Figure 1). This

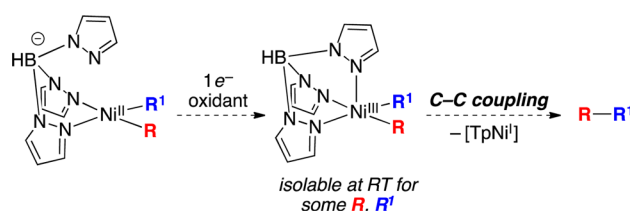


**Figure 1.** Proposed synthesis and reactivity studies of isolable diorgano-Ni<sup>III</sup> compounds.

Article details the design, synthesis, characterization, and reactivity studies of these Ni<sup>III</sup> complexes, which are shown to participate in both C(sp<sup>2</sup>)–C(sp<sup>2</sup>) and C(sp<sup>3</sup>)–C(sp<sup>2</sup>) coupling reactions.

## RESULTS AND DISCUSSION

**Design Considerations.** We sought to prepare isolable Ni<sup>III</sup>(R)(R') complexes bearing carbon donor ligands with varied hybridizations and electronic properties in order to compare their structures and reactivities. We anticipated that two key features would be necessary to achieve this goal. First, we selected the strongly electron-donating tridentate tris-

**Received:** October 3, 2016

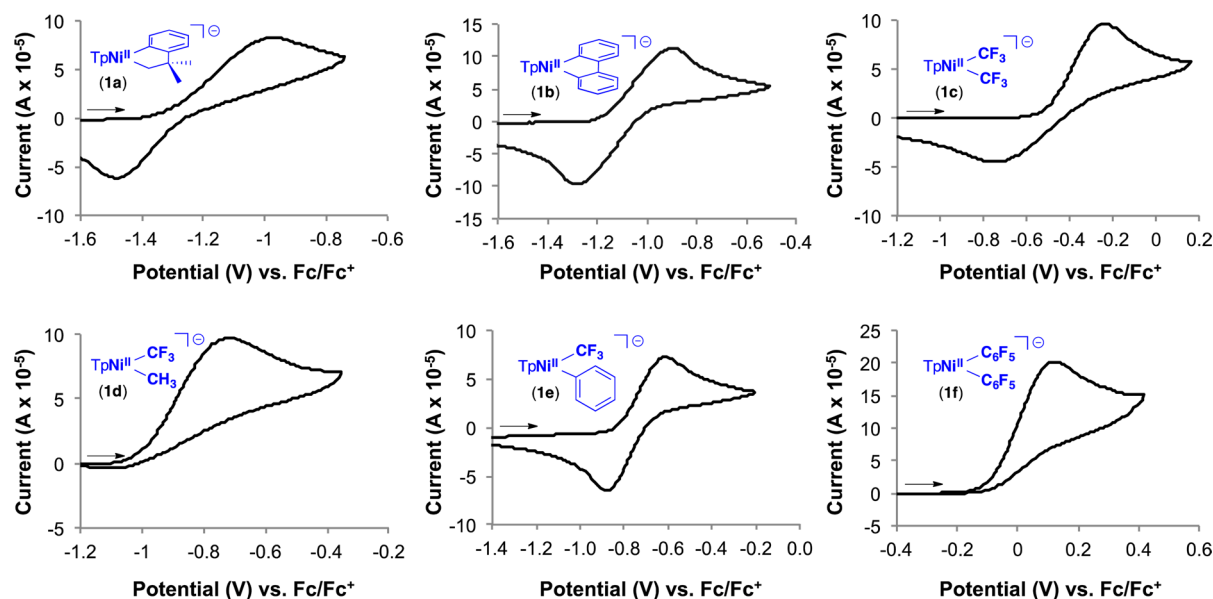


**Figure 2.** Cyclic voltammograms of  $\text{Ni}^{\text{II}}$  complexes **1a–f**. Conditions:  $[\text{Ni}] = 0.01 \text{ M}$ ,  $[\text{NBu}_4\text{PF}_6] = 0.1 \text{ M}$  in MeCN; scan rate =  $100 \text{ mV/s}$ .

(pyrazolyl)borate (Tp) as a supporting ligand, based on our previous work demonstrating that it stabilizes related organometallic  $\text{Ni}^{\text{IV}}$  complexes.<sup>11</sup> Second, we chose carbon donor ligands (R and  $\text{R}^1$ ) that are deactivated toward C–C bond-forming reductive elimination.<sup>12</sup> On the basis of these two criteria, we prepared a series of  $\text{TpNi}^{\text{II}}$  precursors (**1a–f**) bearing either cyclometalated carbon ligands (**1a** and **1b**) or electronically deactivating perfluorinated ligands (**1c–f**) (Figure 2). Importantly, carbon–carbon coupling reactions involving the ligands in complexes **1a–f** are known to be slow or not feasible at  $\text{Ni}^{\text{II}}$  centers.<sup>12</sup>

**Initial Stability Investigations.** The  $1\text{e}^-$  oxidation of  $\text{TpNi}^{\text{II}}$  complexes **1a–f** was first evaluated using cyclic voltammetry (CV). We anticipated that complexes exhibiting quasi-reversible  $1\text{e}^-$  oxidations by CV were most likely to form stable  $\text{Ni}^{\text{III}}$  complexes upon chemical oxidation. As shown in Figure 2, compounds **1a–c** and **1e** show quasi-reversible  $1\text{e}^-$  oxidative waves at a scan rate of  $100 \text{ mV/s}$  ( $i_{\text{pc}}/i_{\text{pa}}$  ranges from 0.2 to 1 in these systems). In contrast, **1d** and **1f** exhibit irreversible  $1\text{e}^-$  oxidations, even at scan rates as high as  $500 \text{ mV/s}$ .

Notably, the CVs of **1a–c** and **1e** all exhibit a large peak-to-peak separation for the  $\text{Ni}^{\text{II/III}}$  couple (260–510 mV). In comparison, a much narrower 76 mV peak-to-peak separation was observed for decamethylferrocene ( $\text{Cp}^*\text{Fe}$ ) when it was added as an internal standard. This indicates that the large peak-to-peak separation is an inherent property of our Ni compounds.<sup>13</sup> It likely results from an electron-transfer chemical (EC) process, wherein the  $1\text{e}^-$  electrochemical oxidation of  $\text{Ni}^{\text{II}}$  to  $\text{Ni}^{\text{III}}$  triggers a change in the Tp binding mode from  $\kappa^2$  to  $\kappa^3$ .<sup>14</sup>

We next examined the chemical oxidation of complexes **1a–f** to generate  $\text{Ni}^{\text{III}}$  products **2a–f** (Figure 3). Ferrocenium tetrafluoroborate ( $\text{FcBF}_4$ ) was selected as the oxidant based on its high solubility as well as its oxidation potential, which is in the range of that required for the  $1\text{e}^-$  oxidation of all of our  $\text{Ni}^{\text{II}}$  complexes. The treatment of **1a–f** with 1 equiv of  $\text{FcBF}_4$  in MeCN at  $-35^\circ\text{C}$  resulted in the rapid disappearance of the diamagnetic  $^1\text{H}$  and  $^{19}\text{F}$  NMR signals of the  $\text{Ni}^{\text{II}}$  starting materials. The in situ analysis of the reactions of **2a–c** and **2e**

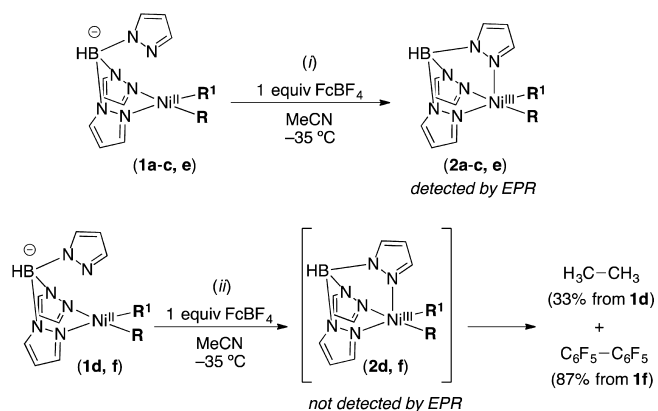


**Figure 3.** (i) Reactions of **1a–c** and **1e** with  $\text{FcBF}_4$  to generate detectable  $\text{Ni}^{\text{III}}$  complexes. (ii) Oxidation of **1d** and **1f** affords C–C coupled products and no detectable  $\text{Ni}^{\text{III}}$  intermediates.

by EPR spectroscopy showed signals consistent with the formation of a  $S = 1/2$   $\text{Ni}^{\text{III}}$  intermediate. In contrast, the oxidations of **1d** and **1f** (conducted at  $-35^\circ\text{C}$  and then immediately frozen at  $-196^\circ\text{C}$ ) did not show detectable  $\text{Ni}^{\text{III}}$  products, as determined by EPR spectroscopy. Instead, products derived from C–C coupling were detected by  $^1\text{H}$  and  $^{19}\text{F}$  NMR spectroscopy (Figure 3, ii). This observation is consistent with the irreversible  $1\text{e}^-$  oxidation waves observed in the CVs of these complexes (Figure 2).

**Isolation and Structural Characterization of  $\text{Ni}^{\text{III}}$  Complexes.** The CV and EPR data are consistent with the formation of  $\text{Ni}^{\text{III}}$  complexes **2a–c** and **2e**. As such, we next pursued the isolation of these compounds. As summarized in Figure 5, analytically pure samples were obtained in 31–87% isolated yield by oxidation of the  $\text{Ni}^{\text{II}}$  precursors with  $\text{AgBF}_4$  ( $E^0 = -0.04 \text{ V vs Fc/Fc}^+$ ). This oxidant was selected because it generates insoluble  $\text{Ag}^0$  as a byproduct. Thus, the  $\text{Ni}^{\text{III}}$  products could be easily isolated via filtration at low temperature and subsequent recrystallization.<sup>15,16</sup>

EPR spectroscopy and effective magnetic moment measurements of **2a–c** and **2e** are consistent with a low spin ( $S = 1/2$ )  $\text{Ni}^{\text{III}}$  electronic structure (see Supporting Information for

complete details). For all four complexes, DFT calculations<sup>17</sup> of the ground-state electronic structure further implicate a radical that is primarily localized on nickel.<sup>18</sup> As shown in Figure 4, the

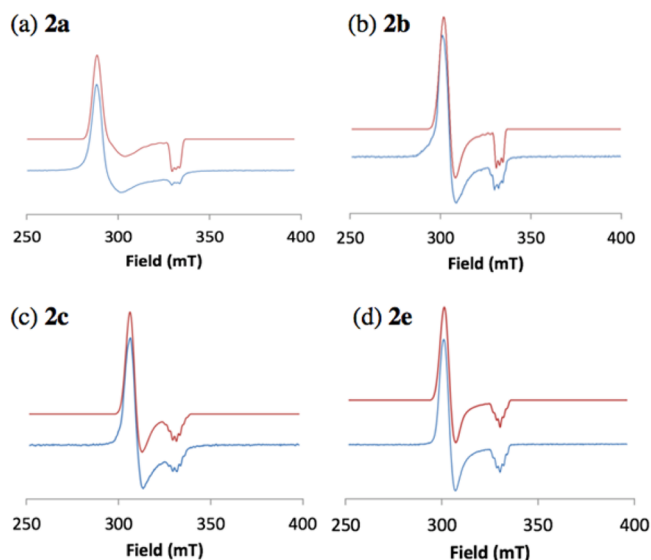


**Figure 4.** Experimental (bottom/blue) and simulated (top/red) EPR spectra for **2a–c** and **2e**: (a) EPR spectrum of **2a** fit using the following parameters:  $g_x = 2.29$ ,  $g_y = 2.25$ ,  $g_z = 2.01$ ,  $A_N = 21$  G. (b) EPR spectrum of **2b** fit using the following parameters:  $g_x = 2.20$ ,  $g_y = 2.19$ ,  $g_z = 2.01$ ,  $A_N = 19$  G. (c) EPR spectrum of **2c** fit using the following parameters:  $g_x = 2.18$ ,  $g_y = 2.15$ ,  $g_z = 2.00$ ,  $A_N(N) = 21$  G,  $A_N(N') = 18$  G. (d) EPR spectrum of **2e** fit using the following parameters:  $g_x = 2.22$ ,  $g_y = 2.19$ ,  $g_z = 2.01$ ,  $A_N(2N) = 18$  G.

EPR spectra of **2a–c** and **2e** in a 3:1 PrCN/MeCN glass at 100 K exhibit hyperfine coupling to one (**2a** and **2b**) or two (**2c** and **2e**) nitrogen atoms. We attribute this difference to the coordination of an acetonitrile ligand in the latter systems to generate octahedral complexes **2c** and **2e-MeCN**.<sup>6b</sup> The presence of the electron-withdrawing CF<sub>3</sub> ligands on **2c** and **2e** likely renders these Ni<sup>III</sup> complexes more electrophilic than **2a** and **2b**.

The Ni<sup>III</sup> complexes **2a–c** and **2e** were also characterized by X-ray crystallography, and an ORTEP structure of each is shown in Figure 5. In all of these compounds, the Tp ligand binds in a  $\kappa^3$ -fashion. The solid-state structures of **2a**, **2b**, and **2e** exhibit a slightly distorted square pyramidal geometry ( $\tau \approx 0.15$ ), while **2c** is octahedral, with a molecule of MeCN occupying the sixth coordination site.<sup>6</sup> Interestingly, while the EPR spectrum of **2e** suggests that a nitrile ligand is bound to the Ni<sup>III</sup> center, attempts to obtain an X-ray quality crystal of the MeCN adduct of **2e** were unsuccessful. Overall, these compounds represent rare examples of structurally characterized diorgano-Ni<sup>III</sup> compounds.<sup>4,6</sup>

**Reactivity of Isolated Ni<sup>III</sup> Complexes.** We next investigated the reactivity of **2a–c** and **2e** toward C–C bond-forming reactions (Table 1). TpNi<sup>III</sup>(CF<sub>3</sub>)<sub>2</sub>(MeCN) (**2c**) proved to be the most thermally robust complex and did not undergo reductive elimination to form CF<sub>3</sub>CF<sub>3</sub> under any of the conditions examined (Table 1, entry 3). Heating a CD<sub>3</sub>CN solution of **2c** for 12 h at 70 °C resulted in the complete consumption of starting material, along with the formation of CF<sub>3</sub>H/D (18%) and [(MeCN)<sub>2</sub>Ni<sup>II</sup>(CF<sub>3</sub>)<sub>2</sub>] (45%) as the major identifiable products. When this reaction was conducted in the presence of 2 equiv of the radical trap TEMPO, TEMPO–CF<sub>3</sub>

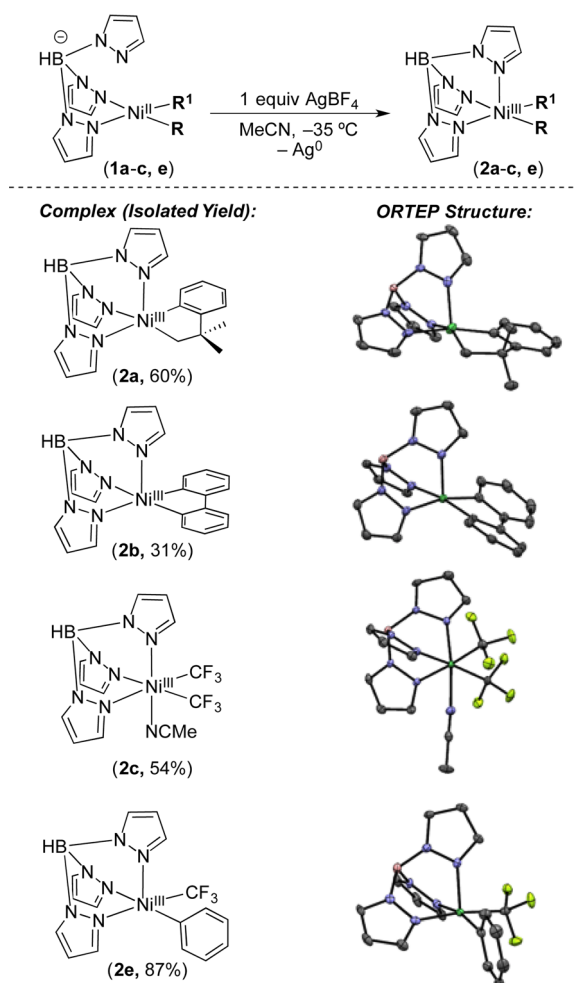


**Figure 5.** Synthesis and ORTEP structures of TpNi<sup>III</sup> complexes **2a–c** and **2e**.

was detected.<sup>19</sup> These results are consistent with a decomposition pathway involving Ni<sup>III</sup>–CF<sub>3</sub> bond homolysis to generate F<sub>3</sub>C•, which can then abstract an H atom from solvent to form CF<sub>3</sub>H or react with TEMPO to generate TEMPO–CF<sub>3</sub>. Notably, both Vici<sup>6b,20</sup> and Mirica<sup>6a</sup> have implicated an analogous pathway in the decomposition of other Ni<sup>III</sup>(CF<sub>3</sub>)<sub>2</sub> complexes.

We next studied the thermal decomposition of the metallacyclic Ni<sup>III</sup> compounds **2a** and **2b**. Heating complex **2a** at 70 °C for 8 h led to C(sp<sup>3</sup>)–C(sp<sup>2</sup>) coupling to generate 3,3-dimethylbenzocyclobutane in 69% yield (Table 1, entry 1). No other identifiable organic fragments were detected by <sup>1</sup>H NMR or GC/MS. Notably, the conditions for this C–C coupling are much milder than those for the related Ni<sup>IV</sup> complex TpNi<sup>IV</sup>(CF<sub>3</sub>) (CH<sub>2</sub>CHMe<sub>2</sub>-*o*-C<sub>6</sub>H<sub>4</sub>), which required heating at 130 °C for 48 h to form 3,3-dimethylbenzocyclobutane.<sup>11a</sup>

The thermolysis of nickelacycle **2b** did not afford the direct C(sp<sup>2</sup>)–C(sp<sup>2</sup>) reductive elimination product, biphenylene. Instead, heating a solution of **2b** in MeCN at 55 °C for 8 h afforded tetraphenylene in 33% yield (Table 1, entry 2). The formation of tetraphenylene is a well-established decomposition pathway for metallacyclofluorenes and could potentially occur via transmetalation between two Ni<sup>III</sup> centers and subsequent reductive elimination.<sup>21,22</sup>

**Table 1.** C–C Coupling from Isolated Ni<sup>III</sup> Complexes **2a–c** and **2e**

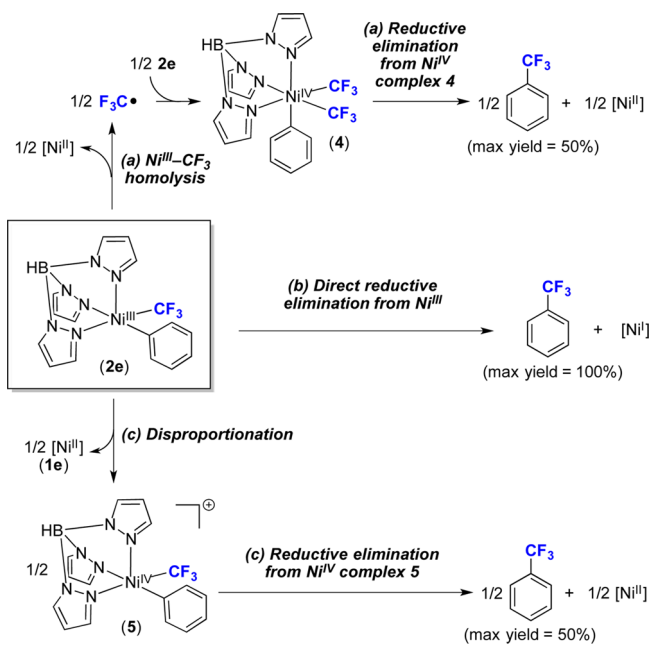
Entry	Ni <sup>III</sup>	Conditions	Organic product <sup>a</sup>	Yield <sup>a</sup>	Yield <b>3</b> <sup>b</sup>
1	<b>2a</b>	70 °C, 8 h		69%	30% <sup>b</sup>
2	<b>2b</b>	55 °C, 8 h		33%	31%
3	<b>2c</b>	70 °C, 12 h	F <sub>3</sub> C–CF <sub>3</sub>	<1%	42%
4	<b>2e</b>	40 °C, 3 h		47%	30%
5	<b>2e</b>	80 °C, 5 min		59% <sup>c</sup>	31%

<sup>a</sup>Yield determined by <sup>19</sup>F or <sup>1</sup>H NMR spectroscopy. <sup>b</sup>Yield based on nickel (maximum is 50%) determined by <sup>11</sup>B NMR spectroscopy. <sup>c</sup>Average of three trials.

Finally, heating a solution of TpNi<sup>III</sup>(Ph)(CF<sub>3</sub>) **2e** in MeCN for 3 h at 40 °C led to complete consumption of starting material and concomitant formation of the C(sp<sup>2</sup>)–CF<sub>3</sub> coupling product, Ph–CF<sub>3</sub>, in 47% yield (Table 1, entry 4). Raising the temperature of the reaction to 80 °C and lowering the reaction time to 5 min resulted in an increase to 59% yield (Table 1, entry 5).<sup>23</sup> Notably, Ph–CF<sub>3</sub> bond-forming reductive elimination is well-known to be challenging from lower oxidation states of nickel.<sup>12c,d</sup> For instance, <5% of Ph–CF<sub>3</sub> was formed when the Ni<sup>II</sup> starting material **1e** was heated for 12 h at 75 °C. As such, these results could ultimately have implications for the development of Ni-catalyzed reactions to form carbon–CF<sub>3</sub> bonds.<sup>1a,c,d,2b</sup>

We also investigated the Ni products of all four of these transformations. No Ni<sup>I</sup> species were detected by EPR spectroscopy in any of these systems. Instead, analysis of the crude reaction mixtures by <sup>1</sup>H and <sup>11</sup>B NMR spectroscopy revealed the presence of Tp<sub>2</sub>Ni<sup>II</sup> (**3**) in 30–42% yield based on nickel (theoretical maximum = 50% yield). This is likely formed via disproportionation and ligand exchange between two TpNi<sup>II</sup> reductive elimination products to yield Ni<sup>0</sup> and Tp<sub>2</sub>Ni<sup>II</sup> (**3**).<sup>11,24</sup> Analogous disproportionation reactions of [Ni<sup>I</sup>] species to form 0.5 equiv of [Ni<sup>II</sup>] and 0.5 equiv of [Ni<sup>0</sup>] have been reported under similar conditions.<sup>5,25</sup> More detailed discussion of the fate of the reduced nickel fragments is provided below.

**Mechanistic Considerations.** We next sought to gain insights into the mechanism of Ph–CF<sub>3</sub> coupling from complex **2e**. As summarized in Scheme 1, there are at least three possible pathways for this transformation. The first (pathway a) involves initial homolysis of the Ni<sup>III</sup>–CF<sub>3</sub> bond followed by reaction of the resulting F<sub>3</sub>C• with a second equivalent of **2e** to yield Ni<sup>IV</sup> complex **4**.<sup>26</sup> Ph–CF<sub>3</sub> reductive elimination from **4** would then release the product. The second (pathway b) involves direct

**Scheme 1.** Possible Mechanisms for Ph–CF<sub>3</sub> Coupling from TpNi<sup>III</sup> Complex **2e**

Ph–CF<sub>3</sub> bond formation from the Ni<sup>III</sup> center. Finally, the third (pathway c) involves the in situ formation of a cationic Ni<sup>IV</sup> intermediate (**5**) via redox disproportionation between two Ni<sup>III</sup> centers. Importantly, the maximum possible yield of Ph–CF<sub>3</sub> in pathway b is 100%, while for pathways a and c it is 50%. As such, the observed yield of 59% provides initial evidence in support of pathway b. Nonetheless, we sought to gain additional data regarding the feasibility of each of the alternate pathways.

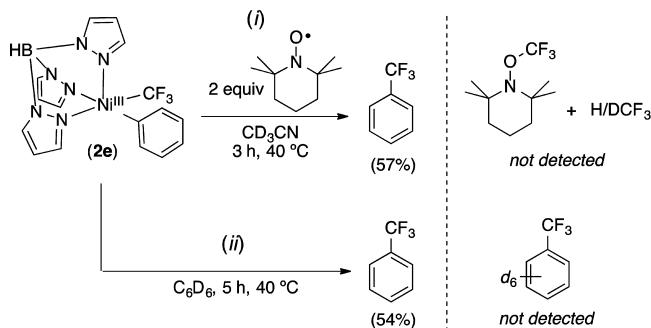
We first interrogated pathway a in more detail. Notably, we have previously isolated Ni<sup>IV</sup> complex **4**, the key intermediate in this pathway, via an alternative synthetic route.<sup>11b</sup> Furthermore, our previous studies showed that Ph–CF<sub>3</sub> bond-forming reductive elimination from **4** requires heating at 55 °C for 14 h (compared to 40 °C for 3 h from **2e**). Thus, if pathway a were operating, we would expect to observe a buildup of intermediate **4** under the milder reaction conditions. However, **4** was not detected when the thermolysis of **2e** was monitored by <sup>19</sup>F NMR spectroscopy, providing further evidence against this pathway.

Two additional experiments were conducted to probe for the intermediacy of F<sub>3</sub>C• in this transformation. First, **2e** was heated in CD<sub>3</sub>CN at 40 °C for 3 h in the presence of 2 equiv of the organic radical trap TEMPO. As shown in Scheme 2, i, the presence of TEMPO did not reduce the yield of Ph–CF<sub>3</sub> under these conditions (47% yield without TEMPO versus 57% yield with TEMPO). Furthermore, neither TEMPO–CF<sub>3</sub> nor H/DCF<sub>3</sub> was detected. Second, the thermolysis of **2e** was conducted in neat C<sub>6</sub>D<sub>6</sub>, which is known to react with F<sub>3</sub>C• to form C<sub>6</sub>D<sub>5</sub>CF<sub>3</sub>.<sup>27</sup> However, the only detectable organic product was C<sub>6</sub>H<sub>5</sub>CF<sub>3</sub> (formed in 54% yield). This experiment demonstrates that the Ph in the organic product is derived from the ligand rather than the solvent. Collectively, these results are inconsistent with mechanism a or any other mechanism involving F<sub>3</sub>C• intermediates.

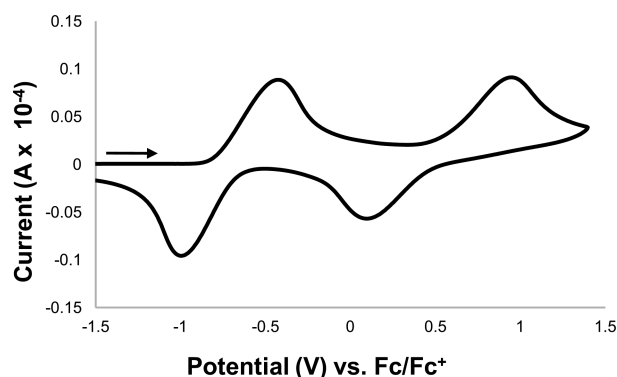
We next investigated the feasibility of Ph–CF<sub>3</sub> coupling via pathway c. A first set of experiments probed the accessibility



## Scheme 2. Radical Trapping Experiments



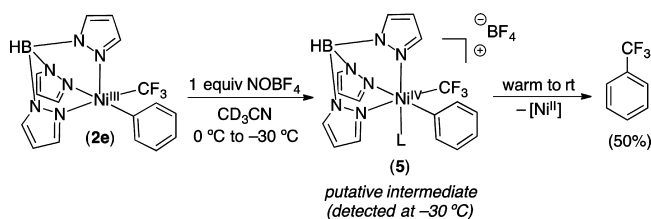
and reactivity of the cationic  $\text{Ni}^{\text{IV}}$  complex **5**, which would be the key intermediate in this disproportionation mechanism. The CV of **1e** at higher potentials reveals a second oxidation with an onset potential of approximately +0.35 V vs  $\text{Fc}/\text{Fc}^+$  (Figure 6). We attribute this to a  $\text{Ni}^{\text{III/IV}}$  couple, which



**Figure 6.** Cyclic voltammogram of **1e** [0.01 M] with 0.1 M  $\text{NBu}_4\text{PF}_6$  in MeCN at a scan rate of 100 mV/s.

interconverts **2e** and proposed cationic  $\text{Ni}^{\text{IV}}$  intermediate **5**.<sup>28</sup> The observed quasi-reversibility of this couple suggests that **5** should be detectable using chemical oxidants with potentials of  $\geq 0.35$  V vs  $\text{Fc}/\text{Fc}^+$ .

To test this possibility, we treated **2e** with 1 equiv of the  $\text{1e}^-$  oxidant  $\text{NOBF}_4$  ( $E^\circ = +0.84$  V vs  $\text{Fc}/\text{Fc}^+$ ).<sup>29</sup>  $^{19}\text{F}$  NMR spectroscopic analysis of the reaction mixture at  $-30^\circ\text{C}$  showed immediate formation of a new resonance at  $-31$  ppm, consistent with the formation of a diamagnetic  $\text{Ni}^{\text{IV}}\text{-CF}_3$  intermediate (Scheme 3).<sup>11</sup> When the temperature was increased to  $25^\circ\text{C}$  over 3 min, this intermediate decayed with concomitant appearance of  $\text{Ph-CF}_3$  (50% yield). While attempts to isolate this compound were unsuccessful, these data are consistent with the formation of  $\text{Ni}^{\text{IV}}$  complex **5**, which undergoes subsequent  $\text{Ph-CF}_3$  reductive elimination.<sup>30</sup>

Scheme 3. Oxidatively Induced  $\text{Ph-CF}_3$  Coupling from **2e** via  $\text{Ni}^{\text{IV}}$  Intermediate **5**

The proposed  $\text{Ni}^{\text{IV}}$  intermediate **5** appears to be accessible from **2e** in the presence of a strong oxidant; however, it remains unclear whether **5** is relevant to  $\text{Ph-CF}_3$  coupling in the absence of an external oxidant. The only oxidant available during the thermolysis of **2e** is a second equivalent of **2e** (Scheme 1); therefore, the maximum yield of  $\text{Ph-CF}_3$  via this pathway would be 50%. As noted above, the yield of  $\text{Ph-CF}_3$  is  $>50\%$  (Table 1, entry 5), indicating that pathway c could not be the exclusive mechanism operating in this system. In addition, redox disproportionation would involve the formation of 0.5 equiv of the starting  $\text{Ni}^{\text{II}}$  complex **1e**, which is expected to be stable and observable by NMR spectroscopy under the reaction conditions. However, **1e** was not detected by  $^1\text{H}$  or  $^{19}\text{F}$  NMR spectroscopy during the thermolysis of **2e** in  $\text{CD}_3\text{CN}$  at  $40^\circ\text{C}$ , again providing evidence against pathway c as the primary mechanism.

Finally, pathway c is expected to exhibit a second order dependence on  $[\text{Ni}]$ , while pathways a and b should be first order in  $[\text{Ni}]$ . The initial rates of  $\text{Ph-CF}_3$  coupling from **2e** were determined in  $\text{C}_6\text{D}_6$  by monitoring the formation of  $\text{Ph-CF}_3$  via  $^{19}\text{F}$  NMR spectroscopy at different concentrations of  $[\text{Ni}]$ .<sup>31</sup> The method of initial rates was then used to determine the order in nickel to be 0.8 ( $R^2 = 0.979$ ; Figure 7). This result

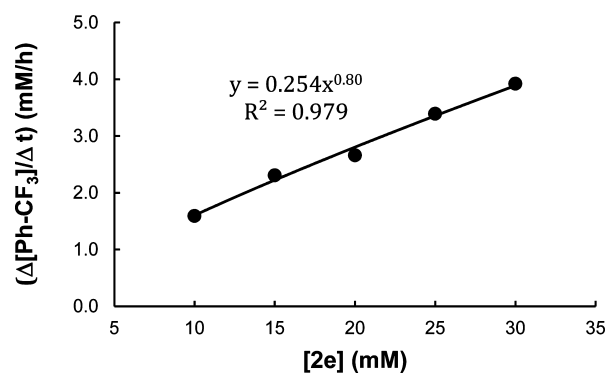


**Figure 7.** A plot of initial rates of  $\text{Ph-CF}_3$  formation versus  $[\text{Ni}]$  for  $\text{Ph-CF}_3$  coupling from **2e** at  $30^\circ\text{C}$  in  $\text{C}_6\text{D}_6$ .<sup>33</sup>

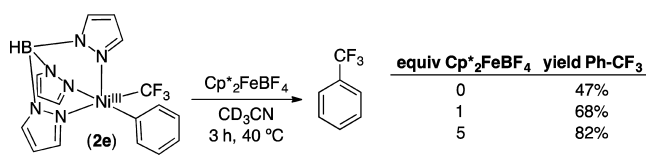
provides further evidence against a redox disproportionation mechanism (or any other pathway that is bimolecular in  $\text{Ni}^{\text{III}}$  before the rate-determining step).<sup>32</sup> Collectively, the available mechanistic data are inconsistent with pathways a and c and support direct reductive elimination from  $\text{Ni}^{\text{III}}$  complex **2e** as the most likely mechanism for  $\text{Ph-CF}_3$  coupling.

A final important consideration is the moderate yield of  $\text{Ph-CF}_3$  and the mass balance in these C–C coupling reactions. Depending on the reaction conditions, the thermolysis of **2e** affords  $\text{Ph-CF}_3$  in yields ranging from 47% to 59% along with small quantities of biphenyl ( $\leq 4\%$ ). We hypothesize that the moderate yields/mass balance are likely due to side reactions promoted by the coordinatively unsaturated low-valent Ni products formed after reductive elimination. There is ample literature precedent for similar issues in stoichiometric reductive elimination reactions from Ni and Pd centers.<sup>34</sup> These are most commonly resolved by the addition of exogenous ligands, which can quench the reactive low valent metal product(s) by saturating open coordination sites. However, in the current system, the addition of exogenous phosphine or pyridine ligands did not improve the yield or mass balance; in fact, these additives generally resulted in diminished yields of  $\text{Ph-CF}_3$ .<sup>35</sup> This result may be due to the

propensity of these ligands to coordinate to the Ni<sup>III</sup> starting material,<sup>36</sup> as there is some literature evidence suggesting that octahedral Ni<sup>III</sup> complexes can have quite different reactivity from their pentacoordinate analogues.<sup>37</sup>

An alternative approach to quench reactive Ni<sup>I</sup> products would involve the addition of a weak oxidant such as decamethylferrocenium tetrafluoroborate (Cp\*<sub>2</sub>FeBF<sub>4</sub>). The potential of this oxidant ( $E^\circ = -0.59$  V vs Fc/Fc<sup>+</sup>) is approximately 0.9 V lower than the onset potential for the oxidation of **2e** to **5** as determined by CV.<sup>15</sup> However, Cp\*<sub>2</sub>FeBF<sub>4</sub> is expected to be capable of oxidizing Ni<sup>I</sup> byproducts to Ni<sup>II</sup> species and could thereby decrease undesired side reactions. Indeed, the addition of 1 equiv of Cp\*<sub>2</sub>FeBF<sub>4</sub> to the thermolysis of **2e** in MeCN (3 h at 40 °C) resulted in an increase from 47% to 68% yield of Ph–CF<sub>3</sub> (Scheme 4). Furthermore, the use of 5 equiv of Cp\*<sub>2</sub>FeBF<sub>4</sub> under otherwise analogous conditions further enhanced the yield of Ph–CF<sub>3</sub> to 82%.

**Scheme 4. Effect of a Weak Oxidant Additive on the Yield of Ph–CF<sub>3</sub> Coupling from **2e****



## SUMMARY AND CONCLUSIONS

In conclusion, this manuscript describes the design, synthesis, characterization, and reactivity studies of a series of stable TpNi<sup>III</sup> complexes bearing C(sp<sup>2</sup>), C(sp<sup>3</sup>), and CF<sub>3</sub> ligands. The synthesis of these Ni<sup>III</sup> complexes was informed by CV studies of their Ni<sup>II</sup> analogues and was ultimately achieved via 1e<sup>−</sup> oxidation with AgBF<sub>4</sub>. The Ni<sup>III</sup> products were isolated and crystallographically characterized. Thermolysis of these Ni<sup>III</sup> complexes resulted in C–C bond formation to liberate organic products, including 3,3-dimethylbenzocyclobutane and Ph–CF<sub>3</sub>. At least three different mechanistic pathways are possible for C–C coupling, including (a) C–C bond formation via free radical intermediates; (b) direct C–C coupling from Ni<sup>III</sup>; (c) redox disproportionation to generate transient Ni<sup>IV</sup> species and subsequent C–C bond-forming reductive elimination from these intermediates. A series of experiments, including the synthesis/reactivity studies of possible Ni<sup>IV</sup> intermediates, rate studies, and radical traps were designed to distinguish between these possibilities for the Ph–CF<sub>3</sub> coupling reaction. Collectively, the data suggest that Ph–CF<sub>3</sub> bond formation occurs via direct C–C coupling from Ni<sup>III</sup>. Furthermore, these studies show that the yield/mass balance of this reaction can be enhanced through the addition of a weak oxidant, which is believed to quench Ni<sup>I</sup> byproducts and thereby minimize undesired side reactions. Overall, these Ni<sup>III</sup> species are potentially relevant to intermediates in Ni-catalyzed cross-coupling, and ongoing work in our lab is focused on the translation of insights gained from these studies into new catalytic methods.

## ASSOCIATED CONTENT

### Supporting Information

The Supporting Information is available free of charge on the ACS Publications website at DOI: 10.1021/jacs.6b10350.

CIF data for **2b** (CIF)

CIF data for **2c** (CIF)

CIF data for **2e** (CIF)

CIF data for **2e-PMe<sub>3</sub>** (CIF)

CIF data for **2a** (CIF)

Experimental details, complete characterization data for all new compounds, and DFT calculations (PDF)

## AUTHOR INFORMATION

### Corresponding Author

\*mssanfor@umich.edu

### ORCID

Melanie S. Sanford: 0000-0001-9342-9436

### Notes

The authors declare no competing financial interest.

C–C Coupling from Isolated Diorgano Ni(III) from @Sanford\_Lab.

## ACKNOWLEDGMENTS

This work was supported by the National Science Foundation (CHE 1361542, CHE 0840456 for X-ray instrumentation, and a graduate fellowship to J.R.B.) and the Australian Research Council. N.M.C. acknowledges the ACS Division of Organic Chemistry for a graduate fellowship. We thank Prof. Nicolai Lehnert for assistance with EPR spectroscopy and Dr. Christo Sevov for helpful discussions. Prof. Michael Hendrich is gratefully acknowledged for assistance with EPR analysis software.

## REFERENCES

- (1) (a) Rosen, B. M.; Quasdorf, K. W.; Wilson, D. A.; Zhang, N.; Resmerita, A.-M.; Garg, N. K.; Percec, V. *Chem. Rev.* **2011**, *111*, 1346. (b) Ge, S.; Hartwig, J. F. *Angew. Chem., Int. Ed.* **2012**, *51*, 12837. (c) Montgomery, J. *Organonickel Chemistry. In Organometallics in Synthesis: Fourth Manual*; Lipshutz, B. H., Ed.; Wiley: Hoboken, NJ, 2013; p 319. (d) Tasker, S. Z.; Standley, E. A.; Jamison, T. F. *Nature* **2014**, *509*, 299. (e) Ananikov, S. *ACS Catal.* **2015**, *5*, 1964.
- (2) (a) Tsou, T. T.; Kochi, J. K. *J. Am. Chem. Soc.* **1979**, *101*, 7547. (b) Hu, X. *Chem. Sci.* **2011**, *2*, 1867. (c) Lipschutz, M. I.; Tilley, T. D. *Angew. Chem., Int. Ed.* **2014**, *53*, 7290.
- (3) For select examples of nickel catalyzed C–C coupling invoking the intermediacy of Ni<sup>III</sup>, see: (a) Jones, G. D.; Martin, J. L.; McFarland, C.; Allen, O. R.; Hall, R. E.; Haley, A. D.; Brandon, R. J.; Konovalova, T.; Desrochers, P. J.; Pulay, P.; Vivic, D. A. *J. Am. Chem. Soc.* **2006**, *128*, 13175. (b) Zultanski, S.; Fu, G. C. *J. Am. Chem. Soc.* **2011**, *133*, 15362. (c) Joshi-Pangu, A.; Wang, C.-Y.; Biscoe, M. R. *J. Am. Chem. Soc.* **2011**, *133*, 8478. (d) Dudnik, A. S.; Fu, G. C. *J. Am. Chem. Soc.* **2012**, *134*, 10693. (e) Dai, Y. J.; Wu, F.; Zang, Z. H.; You, H. Z.; Gong, H. G. *Chem. - Eur. J.* **2012**, *18*, 808. (f) Schley, N. D.; Fu, G. C. *J. Am. Chem. Soc.* **2014**, *136*, 16588. (g) Aihara, Y.; Tobisu, M.; Fukumoto, Y.; Chatani, N. *J. Am. Chem. Soc.* **2014**, *136*, 15509. (h) Wu, X.; Zhao, Y.; Ge, H. *J. Am. Chem. Soc.* **2014**, *136*, 1789. (i) Tellis, J. C.; Primer, D. N.; Molander, G. A. *Science* **2014**, *345*, 433. (j) Zuo, Z.; Ahneman, D. T.; Chu, L.; Terrett, J. A.; Doyle, A. G.; MacMillan, D. W. C. *Science* **2014**, *345*, 437. (k) Cornella, J.; Edwards, J. T.; Qin, T.; Kawamura, S.; Wang, J.; Pan, C.-M.; Gianatassio, R.; Schmidt, M. A.; Eastgate, M. D.; Baran, P. S. *J. Am. Chem. Soc.* **2016**, *138*, 2174.
- (4) During the revision of this manuscript, Mirica and co-workers reported diorgano-Ni<sup>III</sup> complexes that undergo C–C coupling: Schultz, J. W.; Fuchigami, K.; Zheng, B.; Rath, N. P.; Mirica, L. M. *J. Am. Chem. Soc.* **2016**, *138*, 12928.
- (5) For in situ detection of a Ni<sup>III</sup>(CH<sub>3</sub>)(aryl) species, see: Zheng, B.; Tang, F.; Luo, J.; Schultz, J. W.; Rath, N. P.; Mirica, L. M. *J. Am. Chem. Soc.* **2014**, *136*, 6499.

- (6) For isolated examples of bis-perfluoroalkyl  $\text{Ni}^{\text{III}}$  that are not reported to undergo C–C coupling, see: (a) Tang, F.; Rath, N. P.; Mirica, L. M. *Chem. Commun.* **2015**, 51, 3113. (b) Yu, S.; Dudkina, Y.; Wang, H.; Kholin, K. V.; Budnikova, V.; Kadirov, M. K.; Vicić, D. A. *Dalton Trans.* **2015**, 44, 19443.
- (7) For a related mono-aryl  $\text{Ni}^{\text{IV}}$  complex, see: Espinosa-Martinez, G.; Ocampo, C.; Park, Y. J.; Fout, A. R. *J. Am. Chem. Soc.* **2016**, 138, 4290.
- (8) (a) Grove, D. M.; van Koten, G.; Zoet, R.; Murrall, N. W.; Welch, A. J. *J. Am. Chem. Soc.* **1983**, 105, 1379. (b) Grove, D. M.; van Koten, G.; Mul, W. P.; van der Zeijden, A. A. H.; Terheijden, J.; et al. *Organometallics* **1986**, 5, 322. (c) Grove, D. M.; van Koten, G.; Mul, P.; Zoet, R.; van der Linden, J. G. M.; Legters, J.; Schmitz, J. E. J.; Murrall, N. W.; Welch, A. J. *Inorg. Chem.* **1988**, 27, 2466. (d) van de Kuil, V. A.; Veldhuizen, Y. S. J.; Grove, D. M.; Zwikker, J. L.; Jenneskens, L. W.; Drenth, W.; Smeets, W. J. J.; Spek, A. L.; van Koten, G. *J. Organomet. Chem.* **1995**, 488, 191. (e) Higgs, A. T.; Zinn, P. J.; Simmons, S. J.; Sanford, M. S. *Organometallics* **2009**, 28, 6142.
- (9) (a) Pandarus, V.; Zargarian, D. *Organometallics* **2007**, 26, 4321. (b) Castonguay, A.; Beauchamp, A.; Zargarian, D. *Organometallics* **2008**, 27, 5723. (c) Spasyuk, D. M.; Zargarian, D.; van der Est, A. *Organometallics* **2009**, 28, 6531. (d) Spasyuk, D. M.; Goresky, S. I.; van der Est, A.; Zargarian, D. *Inorg. Chem.* **2011**, 50, 2661. (e) Mougang-Soumé, B.; Belanger-Gariépy, F.; Zargarian, D. *Organometallics* **2014**, 33, 5990.
- (10) Tsou, T. T.; Kochi, J. K. *J. Am. Chem. Soc.* **1978**, 100, 1634.
- (11) (a) Camasso, N. M.; Sanford, M. S. *Science* **2015**, 347, 1218. (b) Bour, J. R.; Camasso, N. M.; Sanford, M. S. *J. Am. Chem. Soc.* **2015**, 137, 8034.
- (12) (a) Eisch, J. J.; Piotrowski, A. M.; Han, K. I.; Krüger, C.; Tsay, Y. H. *Organometallics* **1985**, 4, 224. (b) Carmona, E.; Gutiérrez-Puebla, E.; Marín, J. M.; Monge, A.; Paneque, M.; Poveda, M. L.; Ruiz, C. J. *Am. Chem. Soc.* **1989**, 111, 2883. (c) Dubinina, G. G.; Brennessel, W. W.; Miller, J. L.; Vicić, D. A. *Organometallics* **2008**, 27, 3933. (d) Jover, J.; Miloserdov, F. M.; Benet-Buchholz, J.; Grushin, V. V.; Maseras, F. *Organometallics* **2014**, 33, 6531. (e) Yamamoto, T.; Abila, M.; Murakami, Y. *Bull. Chem. Soc. Jpn.* **2002**, 75, 1997.
- (13) The CV scan rate had minimal impact on peak-to-peak separation or peak height ratio in these systems. See [Supporting Information](#) for complete CV data.
- (14) Geiger, W. E. *Organometallics* **2007**, 26, 5738.
- (15) Connelly, N. G.; Geiger, W. E. *Chem. Rev.* **1996**, 96, 877.
- (16)  $\text{Ag}^{\text{I}}$  salts also have been used previously to oxidize  $\text{Ni}^{\text{II}}$  complexes to  $\text{Ni}^{\text{III}}$ . See refs [6a](#) and [6b](#).
- (17) Frisch, M. J.; Trucks, G. W.; Schlegel, H. B.; Scuseria, G. E.; Robb, M. A.; Cheeseman, J. R.; Scalmani, G.; Barone, V.; Mennucci, B.; Petersson, G. A.; Nakatsuji, H.; Caricato, M.; Li, X.; Hratchian, H. P.; Izmaylov, A. F.; Bloino, J.; Zheng, G.; Sonnenberg, J. L.; Hada, M.; Ehara, M.; Toyota, K.; Fukuda, R.; Hasegawa, J.; Ishida, M.; Nakajima, T.; Honda, Y.; Kitao, O.; Nakai, H.; Vreven, T.; Montgomery, J. A., Jr.; Peralta, J. E.; Ogliaro, F.; Bearpark, M.; Heyd, J. J.; Brothers, E.; Kudin, K. N.; Staroverov, V. N.; Kobayashi, R.; Normand, J.; Raghavachari, K.; Rendell, A.; Burant, J. C.; Iyengar, S. S.; Tomasi, J.; Cossi, M.; Rega, N.; Millam, J. M.; Klene, M.; Knox, J. E.; Cross, J. B.; Bakken, V.; Adamo, C.; Jaramillo, J.; Gomperts, R.; Stratmann, R. E.; Yazyev, O.; Austin, A. J.; Cammi, R.; Pomelli, C.; Ochterski, J. W.; Martin, R. L.; Morokuma, K.; Zakrzewski, V. G.; Voth, G. A.; Salvador, P.; Dannenberg, J. J.; Dapprich, S.; Daniels, A. D.; Farkas, O.; Foresman, J. B.; Ortiz, J. V.; Cioslowski, J.; Fox, D. J. *Gaussian 09*, revision A.02; Gaussian, Inc.: Wallingford, CT, 2009.
- (18) Computation employed the ucam-B3LYP functional for geometry optimization utilizing the SDD basis set on Ni and the 6-31G(d) basis set for other atoms. Spin densities > 0.02 are noted at Ni (1.00 to 1.18),  $N_{\text{axial}}$  (0.07 to 0.09),  $N_{\text{MeCN}}$  (−0.05), C bonded to Ni (−0.05 to −0.18). See [Supporting Information](#) for full details.
- (19) TEMPO– $\text{CF}_3$  was found to decompose under these conditions. As such, the observed yield of TEMPO– $\text{CF}_3$  at the end of the reaction (4%) is likely not representative of the total amount of TEMPO– $\text{CF}_3$  formed throughout the reaction.
- (20) Zhang, C. P.; Wang, H.; Klein, A.; Biewer, C.; Stimat, K.; Yamaguchi, Y.; Xu, L.; Gomez-Benitez, V.; Vicić, D. A. *J. Am. Chem. Soc.* **2013**, 135, 8141.
- (21) Xu, H.; Dicciani, J. B.; Katigbak, J.; Hu, C.; Zhang, Y.; Diao, T. *J. Am. Chem. Soc.* **2016**, 138, 4779.
- (22) For the formation of tetraphenylene from metallacyclofluorenes, see: (a) Schwager, H.; Spyroudis, S.; Vollhardt, K. P. C. *J. Organomet. Chem.* **1990**, 382, 191. (b) Edelbach, B. L.; Lachicotte, R. J.; Jones, W. D. *J. Am. Chem. Soc.* **1998**, 120, 2843. (c) Simhai, N.; Iverson, C. N.; Edelbach, B. L.; Jones, W. D. *Organometallics* **2001**, 20, 2759. (d) Beck, R.; Johnson, S. A. *Chem. Commun.* **2011**, 47, 9233.
- (23) The other identifiable organic product of this reaction is biphenyl, which is formed in  $\leq 4\%$  yield, depending on the reaction conditions.
- (24) Gray and black precipitates consistent with  $\text{Ni}^0$  were observed in these reactions.
- (25) Han, R.; Hillhouse, G. L. *J. Am. Chem. Soc.* **1997**, 119, 8135.
- (26) Alternatively, a  $\text{CF}_3$  ligand could be transferred directly from 1 equiv of **2e** to a second equiv of **2e** to form **4**, without the intermediacy of  $\text{F}_3\text{C}^\bullet$ .
- (27) Shi, G.; Shao, C.; Pan, S.; Yu, J.; Zhang, Y. *Org. Lett.* **2015**, 17, 38.
- (28) The wide peak-to-peak separation of 856 mV is likely due to an electron-transfer chemical (EC) reaction mechanism, wherein oxidation to  $\text{Ni}^{\text{IV}}$  triggers the association of a solvent molecule to form a more stable octahedral product.
- (29) Notably,  $\text{NOBF}_4$  was very recently used by Mirica for converting organometallic  $\text{Ni}^{\text{III}}$  complexes to their  $\text{Ni}^{\text{IV}}$  analogues (ref 4).
- (30) The addition of acetylferrocenium tetrafluoroborate ( $\sim 0.3$  V vs  $\text{Fc}/\text{Fc}^+$ ) also induced  $\text{Ph}-\text{CF}_3$  coupling from **2e** at room temperature (in 98% yield). However, oxidation with this oxidant was slow and no  $\text{Ni}^{\text{IV}}$  intermediates were detected by  $^{19}\text{F}$  NMR spectroscopy.
- (31) The initial rates studies were conducted in benzene rather than MeCN because the reaction affords comparable yield (54%) in benzene but is cleaner (i.e., affords fewer minor side products). The addition of 15 equiv of MeCN to the reaction of **2e** in benzene had minimal impact on the initial rate of this reaction (rate =  $2.66 \times 10^{-7}$  mM/h without MeCN and  $2.42 \times 10^{-7}$  mM/h with MeCN at 0.02 M concentration of **2e**).
- (32) We are unable to rule out a mechanism wherein a rate-determining ligand dissociation precedes disproportionation. However, the >50% yield observed at high temperature and the absence of **1e** in the reaction mixture are inconsistent with this pathway.
- (33) An order of 0.8 is also obtained when these data are processed as a log–log plot. See [Figure S21b](#).
- (34) (a) Mann, G.; Shelby, Q.; Roy, A. H.; Hartwig, J. F. *Organometallics* **2003**, 22, 2775. (b) Mann, G.; Baranano, D.; Hartwig, J. F.; Rheingold, A. L.; Guzei, I. A. *J. Am. Chem. Soc.* **1998**, 120, 9205. (c) Pérez-Temprano, M. H.; Racowski, J. M.; Kampf, J. W.; Sanford, M. S. *J. Am. Chem. Soc.* **2014**, 136, 4097. (d) Racowski, J. M.; Dick, A. R.; Sanford, M. S. *J. Am. Chem. Soc.* **2009**, 131, 10974.
- (35) The addition of 3 equiv of pyridine,  $\text{PPh}_3$ , and  $\text{PMe}_3$  to the thermolysis of **2e** led to 33%, 40%, and 1% of  $\text{Ph}-\text{CF}_3$ , respectively.
- (36) The recrystallization of **2e** in the presence of  $\text{PMe}_3$  yielded the corresponding octahedral  $\text{PMe}_3$ -ligated **2e**, as determined by X-ray crystallography (see [Supporting Information](#)).
- (37) For example, during the revision of this manuscript, Mirica reported that C–C reductive elimination from the octahedral complex ( $\text{N}^+$ ) $\text{Ni}^{\text{III}}(\text{CH}_2\text{CMe}_2\text{-}o\text{-C}_6\text{H}_4)$  is very low yielding ( $\sim 10\%$  yield of 3,3-dimethylbenzocyclobutane; ref 4). When compared to the reactivity of **2a**, this suggests that the reactivity of octahedral  $\text{Ni}^{\text{III}}$  complexes may be different from their five-coordinate analogues.